AD-A173 068 STUDY OF MEAN FREE PATH EFFECTS ON GROWTH OF ULTRAFINE METALLIC AEROSOLS(U) RESEARCH TRIANGLE INST RESEARCH TRIANGLE PARK NC P A LAWLESS 31 JUL 86 1/1

UNCLASSIFIED AFOSR-TR-86-0943 F49620-84-C-0017 F/G 7/4 NL

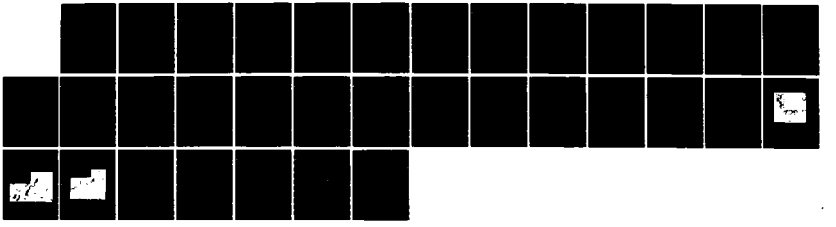

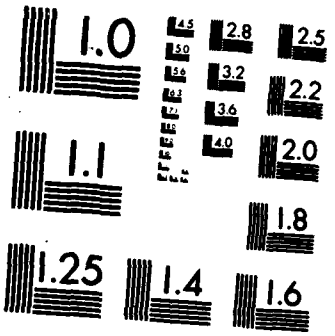

RESEARCH TRIANGLE INSTITUTE July 1986

Study of Mean Free Path Effects on Growth of Ultrafine Metallic Aerosols

Year Two

Work performed under
AFOSR Contract Number F49620-84-C-0017

Prepared for
Air Force Office of Scientific Research
Bolling Air Force Base
Washington, DC

Prepared by
Research Triangle Institute
P.O. Box 12194
Research Triangle Park, NC 27709

Principal Investigator
Dr. Philip A. Lawless

Unclassified
SECURITY CLASSIFICATION OF THIS PAGE

AD-A173068

REPORT DOCUMENTATION PAGE

1a. REPORT SECURITY CLASSIFICATION	1b. RESTRICTIVE MARKINGS
2a. SECURITY CLASSIFICATION AUTHORITY	3. DISTRIBUTION / AVAILABILITY OF REPORT
2b. DECLASSIFICATION / DOWNGRADING SCHEDULE	Approved for public release; distribution unlimited.
4. PERFORMING ORGANIZATION REPORT NUMBER(S)	5. MONITORING ORGANIZATION REPORT NUMBER(S) AFOSR-TR- 86-0943
6a. NAME OF PERFORMING ORGANIZATION: Research Triangle Institute; 6b. OFFICE SYMBOL (If applicable): CAT	7a. NAME OF MONITORING ORGANIZATION: Air Force Office of Scientific Research
6c. ADDRESS (City, State, and ZIP Code): P.O. Box 12194, Research Triangle Park, NC 27709	7b. ADDRESS (City, State, and ZIP Code): Building 410, Bolling AFB, DC 20332
8a. NAME OF FUNDING / SPONSORING ORGANIZATION: AFOSR; 8b. OFFICE SYMBOL (If applicable): NE	9. PROCUREMENT INSTRUMENT IDENTIFICATION NUMBER: F49620-84-C-0017
8c. ADDRESS (City, State, and ZIP Code): same as 7b	10. SOURCE OF FUNDING NUMBERS: PROGRAM ELEMENT NO. 61102F; PROJECT NO. 2306; TASK NO. A2; WORK UNIT ACCESSION NO.

11. TITLE (Include Security Classification)
Study of Mean-Free Path Effects on Growth of Ultrafine Metallic Aerosols (Unclassified)

12. PERSONAL AUTHOR(S)
Lawless, Philip Austin

13a. TYPE OF REPORT	13b. TIME COVERED	14. DATE OF REPORT (Year, Month, Day)	15. PAGE COUNT
Annual	FROM 85 May 1 TO 86 Jun 30	86 July 31	30

16. SUPPLEMENTARY NOTATION

17. COSATI CODES		
FIELD	GROUP	SUB-GROUP

18. SUBJECT TERMS (Continue on reverse if necessary and identify by block number)
Aerosols, metallic aerosols, growth of aerosols, mean-free path, reduced pressure, exoatmospheric

19. ABSTRACT (Continue on reverse if necessary and identify by block number)

This is a report of Year Two activities on a study of metallic aerosol growth under reduced pressure conditions. The aerosol produced is very complex in shape, and the use of fractal descriptors was investigated. The report details the kind of fractal analysis used. It shows that the particles have fractal characteristics which describe stages of growth and that the pressure under which the particles are grown does influence the growth structure. At very low pressures, the particles formed by the exploding wire generator appear to evaporate before they can solidify.

20. DISTRIBUTION / AVAILABILITY OF ABSTRACT ☐ UNCLASSIFIED/UNLIMITED ☐ SAME AS RPT. ☐ DTIC USERS	21. ABSTRACT SECURITY CLASSIFICATION
22a. NAME OF RESPONSIBLE INDIVIDUAL	22b. TELEPHONE (Include Area Code) / 22c. OFFICE SYMBOL

DD FORM 1473, 84 MAR — 83 APR edition may be used until exhausted. All other editions are obsolete.

SECURITY CLASSIFICATION OF THIS PAGE

STUDY OF MEAN FREE PATH EFFECTS

ON GROWTH OF ULTRAFINE METALLIC AEROSOLS

AFOSR F49620-84-C-0017

Year Two Report

1.0 INTRODUCTION

This is a three year project for investigating the dynamics of aerosol formation in gaseous atmospheres ranging from conditions at the earth's surface to those in the extreme upper atmosphere. The research involves theoretical and experimental determination of the behavior of ultrafine aerosol particles at high concentrations. The normal diffusion-limited coagulation and growth of aerosols is expected to be strongly modified as the particle diameter and the interparticle separation approach the mean free path of the gas molecules.

In the first year, the experimental facility was set up, using an exploding wire generator for the production of high concentrations of metallic aerosols. The experiments were devoted to development of sampling methods for the reduced atmosphere environment, and then to the observation of the types of behavior exhibited by single component aerosols.

The types of aerosols generated were highly irregular in appearance, consisting of branched chains of small, spherical particles. The irregular appearance lead us to consider the application of fractal mathemetics for describing the particles and the physical processes behind their growth.

Much of the second year's efforts were devoted to the fractal analysis of the aerosols, and the interpretation of the results. Fractal analysis

is still in an embryonic state with regard to applications in physical measurements, and the techniques used in one situation may not be the best to use in another. In the first year's report, one technique for determining fractal dimension, tiling, was described. Further investigations showed that the tiling approach produced results difficult to interpret consistently, and other fractal measures were examined. This report summarizes our findings to date on using the fractal dimension to characterize growth processes and resulting aerosol particles at atmospheric and lower pressures.

A-1

2.0 THEORETICAL APPLICATION OF FRACTALS TO PARTICLE GROWTH.

Although condensation and growth of aerosols in the liquid state were treated theoretically in the first year's work [1], the observation of solid particle growth quickly lead us to halt that line of investigation. Liquid effects are important during the first few seconds of growth, and for longer times at lower pressures, but are not relevant for most of the aerosol growth we have observed. Instead, we have concentrated on learning the aspects of solid aerosol growth that can be explained with fractal descriptors. (We use some of the growth theory described in [1] to explain the problems of forming aerosol at low pressures.)

Fractals are self-similar geometrical figures that are scale invariant; they have the same appearance no matter what the scale of viewing is. Mathematical fractals, generated by some reproduction algorithm, have an infinite range of scale invariance; natural fractals, generated by some small-scale random process, have only a limited range of scale invariance and are only statistically self-similar.

These differences between mathematical and natural fractals seem to hinder acceptance of fractals in some parts of the scientific community, and most of the fractal applications have been either very theoretical, or very practical (as in the generation of video scenery or effects.) Our point of view is that fractals are useful as quantifiers for particle properties that are difficult to describe in other ways.

Natural fractal objects should be characterized by the range over which a specific fractal behavior holds, and by a fractal dimension. The fractal dimension is a non-integer dimension used to describe the space filling properties of the object. The range of lengths for which a fractal dimension is constant should be sensitive to the conditions under which the particles are formed, particularly with the gas pressure and mean free

path, and indeed, we have found clear changes with gas pressure. There are various ways to define the fractal dimension, depending upon the type of property being measured.

In our use of fractals, we started with a tiling method, described in [1], but had difficulty interpreting the results. A tile could be counted as occupied either if a large fraction of it contained image pixels, or a very small fraction. The resulting fractal dimensions were quite different, depending on the occupancy rule. Tiling may prove useful in the future as an economical way to obtain mass and perimeter information at the same time, but for now it has been set aside.

2.1 Perimeter Method

The next method tested was the perimeter method (also called the equipaced circumscribing polygon method or external hull method). In this method, the perimeter of an object is estimated by counting the number of steps of a given size required to circumscribe the object, and plotting it against the step size on a log-log plot. The fractal dimension of the perimeter is 1-|m|, where m is the slope of the plot, assuming that there is a sufficiently long linear region to say the object is indeed fractal in nature. An equation for expressing the perimeter as a function of the step size is:

$$P(r) \sim r^{1-D}. \qquad (2\text{-}1)$$

where D is the fractal dimension, between 1 and 2 in 2 dimensions. The three dimensional analog would have a D between 2 and 3.

The perimeter fractal does not take into account an object with interior perimeters, such as we see frequently in our micrographs. Furthermore, the perimeter fractal is not easily suited to computer

analysis, which we wanted to implement. On the other hand, the perimeter fractal does seem to be useful in picking out changes of shape between the primary spheres making up an object and the general shape of the object itself. At small scales, the perimeter approaches the geometric perimeter of the circles making up the particle image, and the fractal dimension is close to 1. At larger scales, the perimeter bridges gaps around the particle, and the structure changes more rapidly with scale, giving a larger fractal dimension. We have observed some particles (see Figure 1) which were much longer along one axis than the other, and these particles show a return to a fractal dimension of 1 at scales between the length of the minor axis and the length of the major axis. Thus, in that range the particle behaves as if it were a one-dimensional structure.

2.2 Dilation Method

A commonly used alternative definition of the fractal dimension is based upon the distribution of mass around the center of mass of the object. If the object is fractal, the mass is given by:

$$M(r) \propto r^{D}. \qquad (2\text{-}2)$$

where D is the fractal dimension, and is less than the spatial dimension. We call this a mass fractal, and the method used to calculate it is the dilation method, because a series of boxes is expanded around the center of mass to determine the mass within each box.

In this case, r represents a "radius" of gyration around the center of mass. This fractal dimension definition is quite intuitive in its application, because it corresponds closely with the fraction of area obscured by a particle. A sparsely distributed particle tends to have a low fractal dimension, closer to 1 than 2, and a densely distributed

particle has a high fractal dimension, approaching 2.

This is illustrated in Figures 2 and 3, showing particles grown at 1.0 and 0.1 atmospheres. At small scales around the center of mass, the particles are clearly chain-like, and the fractal dimensions 1.27 and 1.24 reflect this characteristic. Both particles show evidence of growth at the ends of the chains, but the fractal dimension of the growth is considerably different for the two particles. The difference is great enough to identify different mechanisms for the growth process, as will be described in section 2.4.

It is accepted practice to use square boxes in the method, but we think that for comparison with other analysis methods, the expansions should be with circles. The difference between using boxes and circles is that the box method confuses the scale, r by a factor of 1.4, blending some parts of the image that are farther from the center than others.

The expansion around the center of mass means that all the small scale information is obtained from the region near the center of mass. This neglects small scale information in other parts of the particle, unless auxiliary expansions are performed over all the particle.

At large scales, approaching the boundaries of the particle, the dilation method approaches a constant mass, the total mass of the particle, and the fractal dimension no longer has meaning. This boundary-limited behavior occurs at smaller scales when expansions are performed around centers other than the center of mass. Boundary effects on the mass fractal must be anticipated in the analysis, and the boundary-limited regions must not be given a fractal interpretation. The boundary regions were not shown in Figures 2 and 3. Both particles are about 2 micrometers long, and the fractal analysis was carried out for box lengths of up to about 1.3 micrometers. Above that size, the boundary effects became

obvious as a flattening of the curve.

2.3 Correlation Method

A method which makes use of all the information in the image is a correlation analysis. The correlation function is a relation describing the relative frequency of finding two parts of the image at a given distance from one another. For fractal objects, the correlation function is related to the fractal dimension by:

$$C(r) \sim r^{D-d}. \qquad (2\text{-}3)$$

where D is the fractal dimension and d is the spatial dimension. Since the fractal dimension is less than the spatial dimension, the correlation function decreases with r.

Programs were written to calculate the correlation function directly, involving scanning the image, multiplying pixel values, and summing at various values for r. The process is manageable for small images and small values of r, but the time consumed in the calculation grows quickly for larger images. The correlation analysis is best performed with FFT methods, and we have obtained a commercial software package with the power to analyse the micrograph images. The software to interface with the FFT has not yet been written. The correlation method does give a very complete picture of the fractal characteristics of the particles at small scales and so far seems to agree well with the dilation method at intermediate scales. This analysis method should improve our ability to extract information from the micrographs more quickly and give a clearer interpretation of the results.

Both the mass and correlation fractals have a similar behavior for a given particle and range of scales. The correlation function itself

decreases with r, but if it is multiplied by r^2, then the result is very similar to the mass fractal:

$$r^2 \bullet C(r) \sim r^{D-d} r^d = r^D, \qquad (2\text{-}4)$$

because d=2 for the images. In this way, it is feasible to use the dilation method to obtain the fractal characteristics at large scales, where it is a fairly efficient technique, and the correlation method at small scales, where it is effective.

There seems to be a fundamental difference between these two measures of fractal dimension and the perimeter method, but it has not been discussed in the literature. For instance, with a circle or disk, the perimeter fractal dimension changes continuously with step size and approaches the limit 1.0, because the perimeter of the circle is one-dimensional. On the other hand, the mass definition of fractal dimension gives a constant value of 2 for any scale up to the circle radius, because the disk is indeed two-dimensional.

Figures 4 - 7 show some comparisons of the perimeter, dilation, and correlation methods for four different particles. The dilation curves were divided by the square of the box length to produce curves analogous to those obtained directly from the correlation and perimeter methods. It can be seen that the dilation and correlation methods give comparable results in the ranges for which there is overlap. The comparison would improve if the scale for the dilation were divided by two to adjust the box side to an equivalent "radius". We think the comparison would improve further if a dilation of circles were used.

The perimeter method shows fair agreement of fractal dimension for some particles over some of the ranges. Because the perimeter fractal is calculated differently from the others, the slopes of the curves are NOT

expected to look the same, and only the dimensions should be compared. However, the perimeter does not always show changes of character, even when the other two do. The two types of measures are in better agreement on particles that do not have interior structures or loops, an indication that the properties being described in the fractal dimension are really quite different.

This difference in interpretation of these two fractal measures caused some difficulty when we attempted to test our mass fractal analysis program with geometrical objects that had been generated as perimeter fractals; the dimensions simply did not match up. For Euclidean objects like a disk, the two dimensions add to 3. For many of our particles, the perimeter fractal dimension and the mass fractal dimension are both about 1.5, also adding to 3 over comparable scales. The relation also holds, but not perfectly, in other particles with higher values of mass fractal dimension.

We are continuing to think about this relation, because it seems clear that there are some properties better described with the perimeter fractal (such as aerodynamic drag) and others better described with the mass fractal (such as weight or obscuring cross-section.) A simple relation connecting them would be very useful.

2.4 Physical Interpretations of Fractal Dimensions

Most of the theoretical descriptions of fractal growth have involved computer simulations of particle collisions under various operating hypotheses. For instance, particles can be assumed to randomly "walk" toward one another, to have degrees of sticking upon collision. Clusters of particles can be allowed to participate in the random walk. These hypotheses have been found to "grow" clusters of particles with fractal character over a considerable range of sizes, and the fractal dimension

depends on the particular process involved.

In particular, using the mass fractal definition, particles which collide with already existing clusters by Brownian diffusion exhibit a fractal dimension of 1.67 (5/3 theoretically). In higher dimensions, this is extended to:

$$D \cong 5/6d \qquad (2\text{-}5)$$

where d is the spatial dimension from 2 to 6 [3,4].

The Brownian collision of clusters with clusters generally leads to a fractal dimension of 1.45 (for d=2) or 1.75 (for d=3) under a wide variety of assumptions, but there does not seem to be an exact value.

Finally, if particle-cluster collisions occur ballistically (straight line trajectories), the fractal dimension is about 1.95, with a theoretical limit of 2 for infinitely small particles. The difference between 1.95 and 2 occurs because of the voids between tightly-packed particles.

When dealing with images of particles (strictly two-dimensional), the question arises of how to relate the results to real three-dimensional particles. One answer is that for sparse particles, in which there is relatively little screening of parts of the image by other parts, the fractal dimension should be increased by 1 in going from 2 to 3 dimensions. Another answer is that the fractal dimension of the particle must obey a relation derived from causality [5]:

$$D_0 \geq d - 1 - D_1. \qquad (2\text{-}6)$$

where D_0 is the particle fractal dimension and D_1 is the fractal dimension of the trajectory of an incoming particle. If the trajectory is Brownian, then D_1 is equal to the space dimension. If it is ballistic, the D_1 is 1. Therefore, the particle fractal dimension must fall between the rather

broad limits of 1 and d.

3.0 EXPERIMENTAL RESULTS

At the end of the first year, we were able to discern several experimental regions of particle growth. By keeping all experimental conditions constant, except for the gas pressure, different modes were observed and could be described qualitatively. Now, we are able to assign quantitative values to the different modes of growth.

In general, our observations are in line with what could be expected from the fractal growth models. When the growing particles were roughly the same size, the growth was similar to cluster-cluster aggregation. As the clusters became large enough to diffuse more slowly, then particle-cluster aggregation was observed. We also have observed ballistic aggregation at two different time and size scales.

3.1 Measured Fractal Dimensions

The exploding wire generator (EWG) produces nearly uniformly sized solid aerosol particles. They are about 0.04 to 0.05 micrometers in diameter, and are similar to particles produced in other EWG devices. Given the power level associated with the formation of these particles, it is likely that we could produce primary particles of about 0.1 micrometers diameter, but that it would be difficult to produce smaller primaries [6]. The critical parameter is the energy per mass of wire exploded, with higher values producing smaller sizes.

At 1.0 and 0.1 atmospheres, the initial growth of the solid aerosol showed fractal dimensions consistent with cluster-cluster growth for dimensions up to about 0.3 micrometers. We interpret this to mean that the primary particles form small clusters of about 0.05 to 0.1 micrometers which diffuse rapidly toward one another. From this scale to about 0.3 micrometers, the clusters are all similarly sized, and have roughly equal

diffusivities. As the clusters grow to larger sizes, they become relatively immobile, but there are still large numbers of 0.05-0.1 micrometer clusters available for continued growth. These smaller clusters can penetrate the structure of the larger clusters much like primary particles and lead to a denser particle form, having a fractal dimension of 1.6 - 1.7 (characteristic of particle-cluster aggregation).

At 0.01 atmosphere, the dilation fractal dimensions at small scales, <0.2-0.5 micrometer, are in the range 1.4-1.7, suggesting that particle-cluster and cluster-cluster aggregation are operative. However, the structure of the particles is noticeably more dense. We think that at this pressure, we see the beginning of ballistic aggregation, heading toward a fractal dimension of 1.9+. The correlation analysis shows fractal dimensions in the range 1.85 to 1.89 for scales near the primary particle size, 0.05 micrometers. At larger scales, the fractal dimension decreases toward the cluster-cluster value as the initially-formed clusters begin to collide.

These differences between the dilation method and the correlation method are important. They indicate that information from the whole particle is needed to infer the operative mechanisms. Even then, some physical interpretation of conditions is needed to sort out the competing effects. If the center of mass of a particle does not contain parts of the particle nearby, then the small scale fractal dimension will be distorted by the lack of mass. Conversely, if the center of mass lies in an unusually solid part of the particle, the mass fractal dimension will overemphasize the solidity at small scales.

We have observed ballistic aggregation in the upper size range, but have not yet completed the measurements. This aggregation occurred at 0.1 atmospheres when the particles grew to sizes of 15 to 20 micrometers. The

largest of the clusters apparently achieved a significant settling velocity and swept through the cloud of smaller particles. The resulting clusters are roughly spherical and appear quite dense in the micrographs. We expect that the mass fractal would be about 1.9 by simple inspection.

This last case of ballistic aggregation may not be of direct interest to the program, but does illustrate that a change of fractal dimension (from about 1.67 to 1.9) can indicate a major change in the process of growth. We hope it can show the size at which the change takes place.

Although the fractal analysis is proving fruitful, there are still some unexplained properties. One of the major ones is that the particles are showing a moderate change in fractal dimension with time, even while the general observations of particle-cluster or cluster-cluster aggregation hold true. This may be due to an initial formation of linear clusters, which then combine relatively linearly. Some of the micrographs reflect this. A process of this sort would lead to an initially low fractal dimension.

Such a process could arise from electric charges on the particles. The charges tend to concentrate at the ends of chains and provide additional attractive forces for other particles or chains. Figures 2 and 3 show possible charge effects at small scales. It seems unlikely that chains would grow in such a nearly linear fashion without some force directing approaching particles to the ends. Computer models of charged particles do produce long chain aggregates. As the clusters grow, the charges could be spread over larger areas and lose their influence, or, if bipolar charges are involved, the charges would neutralize one another. This will remain an area for further investigation.

Another troublesome area is that the fractal dimensions by correlation and dilation do no agree as closely as we think they should, especially as

given by Equation 2-4. Part of the problem is associated with the dilation method's use of square boxes, rather than circles, and we intend to refine that calculation in the near future.

The last problem is that, although we see general trends in the growth mechanisms as functions of pressure, we are as yet unable to see a clear change in the particle's structure as a function of the gas mean free path. We hope that the scales at which the structure changes from one type of aggregation to another would show a dependence on mean frec path. So far the relationship has not been clear.

3.2 Low Pressure Problems

At the next lower decade in pressure, 0.001 atmosphere, we repeatedly failed to generate and observe any particles at all. This led us to perform a series of experiments at intermediate pressures to determine the level at which particle generation did resume. For the quantity of wire we use, that occurred at 0.002 atmosphere. We have addressed this problem on theoretical grounds, looking in more detail at the exploding wire process.

The details of the explosion follow the steps listed below [7].

1. The flow of current heats the wire to its melting point. Inertia and magnetic fields contain the molten wire and allow current to continue flowing.

2. The wire is heated well above is vaporization point. It is superheated, because the time scale is too short for equilibrium boiling. In a reduced gas pressure, it may not heat to the same temperature as in a high pressure atmosphere.

3. Vapor pockets form in the liquid, but heating continues as long as there is a continuous path in the liquid.

4. Vaporization disrupts the current flow. The remaining liquid filaments coalesce into spherical droplets.

5. Thermionic emission causes the droplets to emit electrons and become positively charged. Because the vapor density is high, electron multiplication is suppressed.

6. The vapor expands rapidly. The liquid droplets are carried into regions of decreasing vapor concentration. In the decreasing vapor, electron multiplication takes place, and the arc may re-strike.

We have observed empirically the charging that results from materials with different melting/boiling points. These differences were used to obtain an aerosol with essentially no charge, and could be used further. It also appears that the restrike phenomenon would be a good indicator of the presence of liberated electrons, and we will pay attention to measuring this in the future.

This analysis of the wire breakup has been supported by high-speed X-ray photographs of wires. The mechanisms leading to breakup may not be unique, but it is clear that some liquid droplets remain from the original wire. It is not totally vaporized by the electrical current.

Now, the superheated liquid droplets expand into the sample chamber where competing processes take place. First, there is cooling by the ambient gas. There is potential continued evaporation of the material from the droplets, and there is potential condensation of metallic vapor onto the droplets.

The minimum radius which can support continuous growth is given by the Kelvin equation:

$$r_c = 2Ms/RTd\ln S. \qquad (3\text{-}1)$$

where:

r_c = particle radius
M^c = molecular weight of metal
s = surface tension of metal (850 dyne/cm)
R = gas constant
T = temperature of metal
d = density of metal
S = saturation ratio [1].

If the radius is less than this critical value, the droplet will ultimately evaporate. If the radius is larger, it will grow. The problem in applying this relation is the great uncertainty about the experimental situation.

Under the steps leading to formation given above, the temperature of the liquid drop must be at least equal to the normal boiling point of silver, 2483 K. If the superheating is substantial, the temperature might be as high as 2600 K. It is also not clear that the ambient pressure could affect this temperature strongly. The saturation ratio is definitely an equilibrium concept: the ratio of ambient partial pressure to the vapor pressure at the surface of the particle.

Calculations of the critical radius over a range of temperatures corresponding to boiling at 0.001 atm up to 7 atm (1560-5040 K) produce a very narrow range of critical sizes. For S = 1.01, the critical radius decreases from 0.18 micrometer to 0.05 micrometer. For S = 1.02, the range is 0.09 to 0.03 micrometer, and for S = 1.05, the range is 0.04 to 0.01. These results are right in the range of primary particles encountered. Any particles formed with smaller radii than these will evaporate. Any larger ones will grow.

These calculations strongly suggest that the failure to produce aerosol particles is due to evaporation of the liquid droplets. The cause of the evaporation may be due to higher temperatures and a slower rate of cooling at the reduced pressures, or to a change in the saturation ratio. The saturation ratio might have to be interpreted in a dynamic sense, as the vapor and particle cloud expands.

We are interested in refining our understanding of this process, because it may indicate that a change of materials would change the lowest pressure for aerosol formation substantially. However, we do not think that changes would lower the critical pressure by much more than one

decade, and are making plans to pursue other avenues for particle generation at lower pressures. Once the particles are generated, the growth should not be so drastically affected by pressure.

Also at the lower pressures, particle settling becomes a major factor in the time available for sampling. Accordingly, we have included a settling sampler on the bottom of the chamber. It consists of sampling stubs covered by a shield plate with a window. The window is closed during the initial explosion and then may be positioned over any stub for variable periods of time. This sampler has been tested and appears to work well. It will be invaluable at lower pressures, and a useful adjunct at the higher pressures.

4.0 SUMMARY AND FORECAST

The next approach we will take in lowering the pressure for generating particles will be to fill the chamber with seed nuclei prior to the explosion. This will alleviate the problem of forming a critical nucleus and will allow the growth by condensation to commence immediately. Seed nuclei can be formed by heating a metallic wire to a temperature that is a major fraction of its melting point. We would not have the same pressure problem with the seed generator as with the main explosion, because the seeds are generated at atmospheric pressure. The chamber is filled with nuclei before pumping it to the explosion pressure. In this way we can control the generation of nuclei to any degree desired.

With seed nuclei, even if the liquid droplets from the wire evaporate, the vapor can condense on the seeds. The number of nuclei will be much smaller than the number formed in an explosion, so the resulting particles should be larger. This assumes that all of the vapor condenses onto them.

Another approach which we will pursue is the use of different wire materials for the explosions material. We are particularly interested in lower melting point materials, because they will disrupt at lower temepratures and pressures than the silver and should not disperse at quite the same rate. We will particularly explore materials which have a smaller critical radius, because they will not be so likely to evaporate. This work should allow us to state general guidelines for the generation of aerosols at reduced pressures, but we may not find materials which will allow direct formation at low pressures.

It is possible that a slight confinement of the explosion, as in a small diameter tube, would allow a substantial reduction in gas pressure. This approach would result in a locally high pressure for a short time and may be an alternate approach to using the seed nuclei.

Covaporization of a metal and another material is part of the projected work in the last year's effort. The reason for doing this is that many aerosol generating schemes always involve binary components, either deliberately or through contamination. In terms of the survivability initiative, it would be particularly interesting to observe the growth of metallic aerosol in conjunction with carbon particles. We think that the shock from the exploding wire would have enough energy to vaporize or shatter a carbon foil wrapped around the wire. This would produce a mixed aerosol environment in which the growth of the metallic aerosol should be substantially modified by the carbon aerosol. The inter-particle forces would be much different; the diffusion rates would be much different; and the primary particle sizes would likely be different.

The fractal analysis methods have been adequate so far, but still need a few refinements. The dilation analysis will be brought closer to the correlation analysis by going to a circle expansion, rather than a box expansion, and both methods will be used in analysing new particles. The relations between two-dimensional analyses and three-dimensional fractal dimensions will be further clarified, and the implications examined for real particles.

We have proposed the study of electric fields on the growth of the aerosols. Metallic aerosols are particularly susceptible to electric field effects, because even electrically neutral particles can experience strong dipole polarization and torques in an electric field. The concentration of electric field at the extremities of a conducting particle leads us to think that the random agglomeration patterns will become much more linear. What is not known is the degree of alignment as a function of field strength. There should be a smooth transition from non-aligned particles to aligned ones as the field strength is increased, and this transition

should show up both in the length of the aerosol particles and in their fractal dimensions. This is one case is which there should be a clear application of the perimeter fractal, because the ultimate form of a chain is a line of dimension 1.

REFERENCES

1. Study of Mean Free Path Effects on Growth of Ultrafine Metallic Aerosols. Year One Report. June 1985.

2. Study of Mean Free Path Effects on Growth of Ultrafine Metallic Aerosols. Year Two Progress Report. March 1986.

3. Meakin, P. Phys. Rev. A **27**, 1:604-607 (1983).

4. Meakin, P. Phys. Rev. Lett. **27**, 3:1495-1507 (1983).

5. Ball, R.C. and Witten, T.A. Phys. Rev. A **29**, 2966-2967 (1984).

6. Phalen, R.F. J. Aerosol Sci. **3**, 395-406 (1972).

7. Chace, W.G. and Moore, H.R. "Exploding Wires, Vol.1" Plenum Press, N.Y. 1958.

PUBLICATIONS

Pseudo-Self-Preserving Particle Size Distribution for Brownian Coagualtion in the Transition Regime. A.S. Damle and P.A. Lawless. Still in preparation for submission.

Mean Free Path Effects on Particle Coagulation. P.A. Lawless, P.C. Reist, and M-T. Hsieh. Proceedings of the 1985 CRDC Scientific Conference on Obscuration and Aerosol Research. (R.H. Kohl, ed.).

Particle Generation by Exploding Wires. P.A. Lawless. Presented at the 1986 CRDEC Scientific Conference on Obscuration and Aerosol Research.

Fractal Analysis of Irregularly Shaped Aerosol Particles Grown at Reduced Pressures. M-T. Hsieh, P.A. Lawless, and P.C. Reist. To be submitted to Aerosol Science and Technology.

Preliminary Study of the Growth of Metallic Aerosols Under Reduced Pressure Environment. Master's Thesis. Ming-Ta Hsieh. University of North Carolina, Chapel Hill (1986).

PROFESSIONAL PERSONNEL

P. A. Lawless, Ph.D. Principal Investigator, Research Triangle Institute

P. C. Reist, Ph.D. Co-Investigator, University of North Carolina

A. S. Damle, Ph.D. Research Triangle Institute.

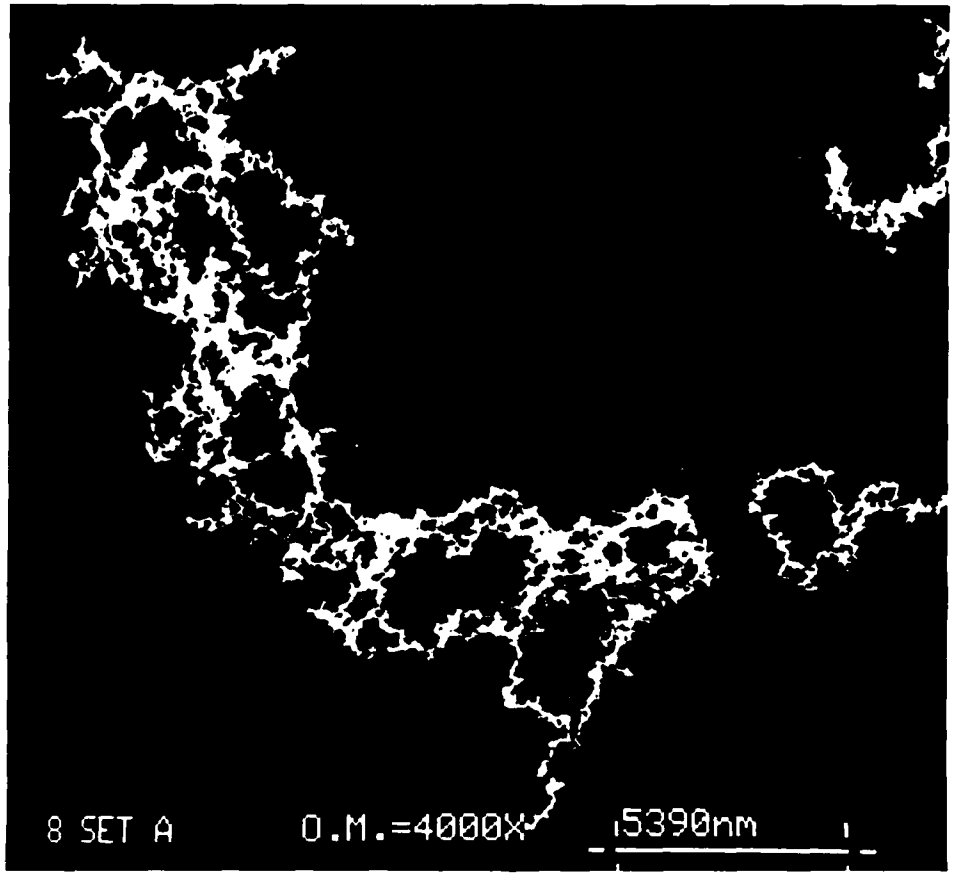

Figure 1. An elongated particle encountered in the measurements.

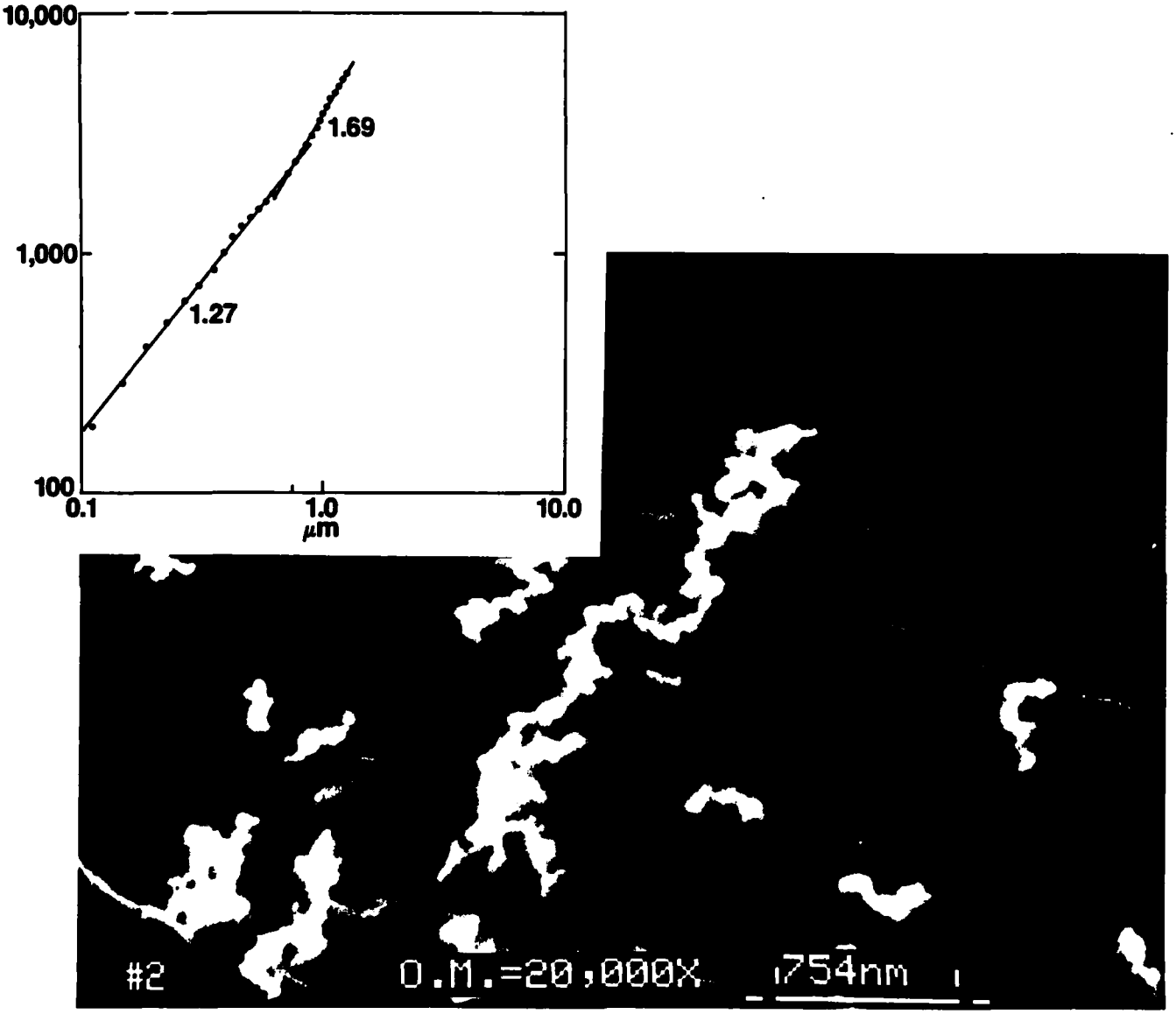

Figure 2. Long particle grown at 1.0 atm. and its fractal dimension.

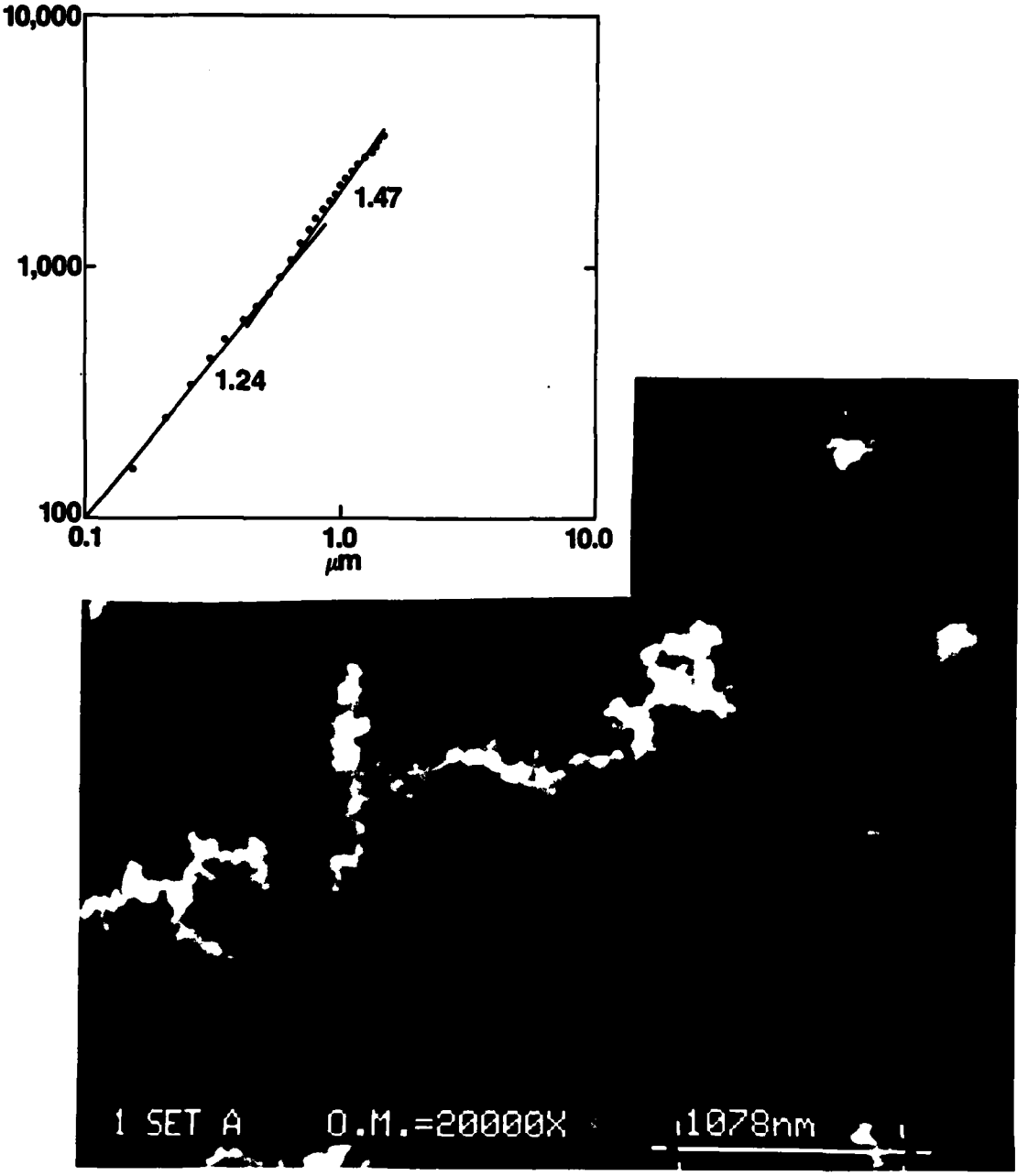

Figure 3. Particle grown at 0.1 atm. and its fractal dimensions.

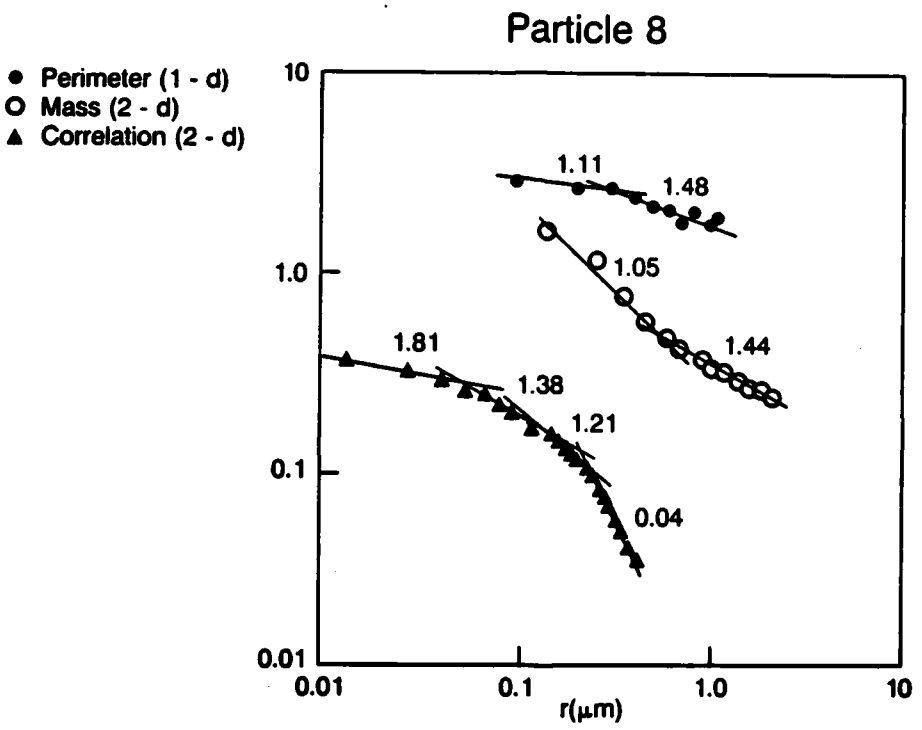

Figure 4. Comparison of perimeter, dilation, and correlation fractals.

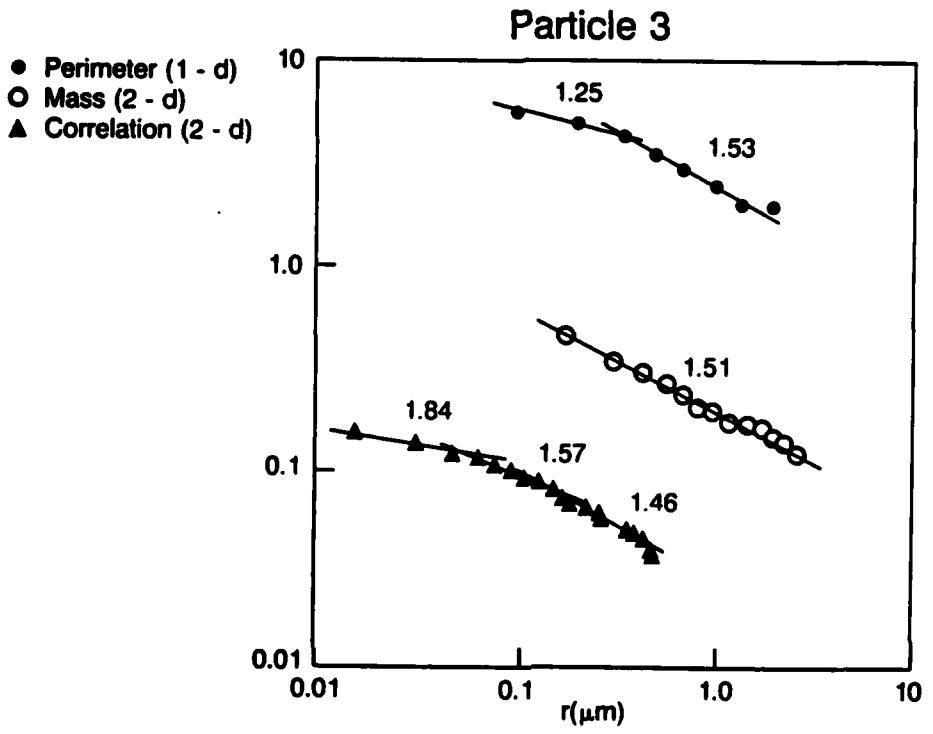

Figure 5. Comparison of methods for another particle.

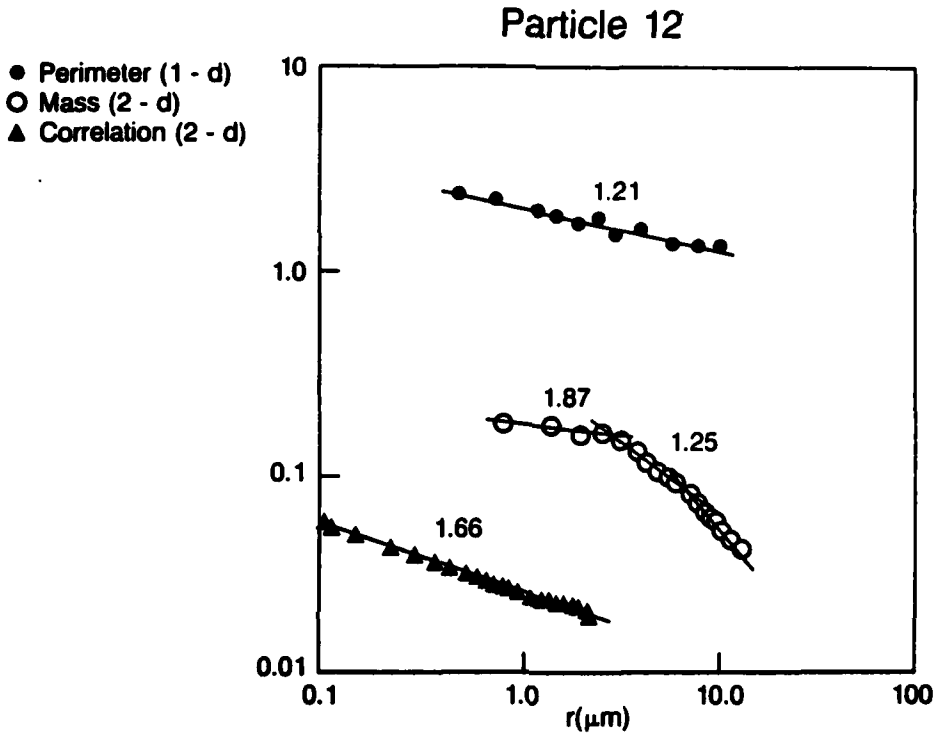

Figure 6. Comparison of methods for a third particle.

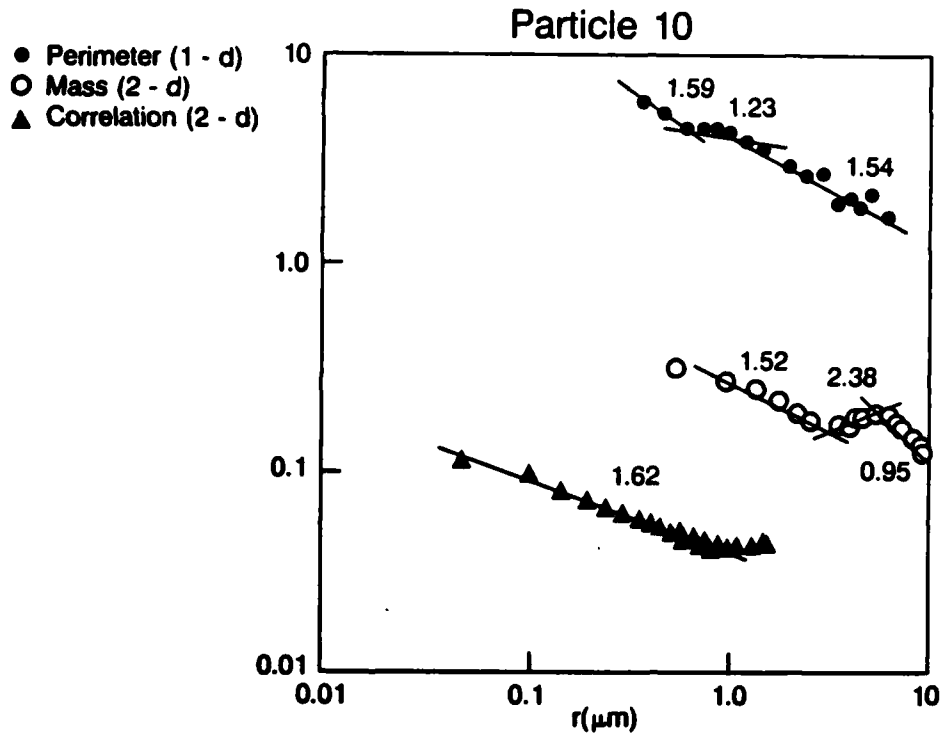

Figure 7. Comparison for a larger particle, where boundary effects are visible.

FMD

12-86

DTIC